Influence of core and hexapod geometry, and local reinforcement on the performance of ultra-lightweight ULE mirror

William R. Arnold[a], H. Philip Stahl[a],
[a]NASA Marshall Space Flight Center, Redstone Arsenal, Huntsville, AL, USA 35812

ABSTRACT

The Habitable Exoplanet Observatory (HabEx) mission has unique optical performance requirements which drive the mirror design process beyond the traditional criteria. While mass and stiffness are still important, the response to inertia loading (expressed in terms of Zernike coefficients) to omni-directional excitation dominates the effort. While a Zerodur mirror is the current baseline, as mass budgets change, a ULE design is being studied as a potential alternative. This trade study looked at over 264 design variations using the Arnold Mirror Modeler and ANSYS© to investigate the influence of various design elements, including: substrate thickness, core cell size, hexapod geometry and local reinforcement. Design 'goodness' was evaluated based on the mirror's inertial deformation response to omni-directional input. This response was calculated via RSSing Zernike polynomial responses to (XYZ) accelerations.

Keywords: HabEx, primary mirror design, trade studies, ULE alternatives

1. INTRODUCTION

The HabEx Architecture-A telescope requires a 4-meter off-axis circular-aperture monolithic primary mirror. An open-back Zerodur mirror is the baseline, with a closed-back ULE mirror as an alternative. This paper is one in a series of design studies supporting the project. Previous papers[1,2] covered the Zerodur option extensively and limited ULE cases as well as discussing the overall scope of the HabEx work at MSFC. This paper expands the ULE design parameters with an emphasis on the impact of suspension system geometry and local reinforcement. The HabEx mission and the unique requirements of the coronagraph control the output format of this study. For HabEx, inertial deformation (response to inertial loads) is an important performance parameter both as it relates to manufacturing for diffraction limited performance and to ultra-stable on-orbit wavefront performance required by coronagraph.

The ranges of all the parameters used in this study are set by published industrial capabilities. The actual mirror manufacturer may or may not be the raw material supplier. A total of 264 separate models were created and run in period of two weeks using the AMM (Arnold Mirror Modeler) and ANSYS.

1.1 Purpose of HabEx

The basic goals of the HabEx Program are explained in Figure 1.

Figure 1: Basic goals of HabEx program

1.2 Baseline HabEx Architecture A Concept

The HabEx Science and Technology Definition Team (STDT) chose the following parameters for Architecture-A (Figure 2). The telescope would have a 4-meter aperture, with a 72-meter external Starshade occulter flying in formation with the satellite. Four instruments would be included on the satellite; a coronagraph instrument for Exoplanet Imaging, a Starshade Instrument for Exoplanet Imaging, a UV-NIR Imaging Multi-object Slit Spectrograph for general observatory science and a High-Resolution UV Spectrograph for general observatory science.

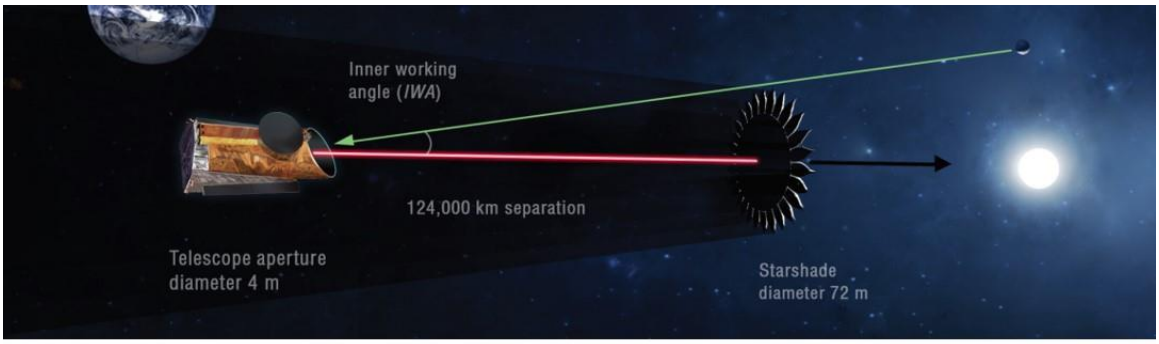

Image from HabEx interim report URS273294 *Pre-Decisional - For Planning Purposes Only*

Figure 2: Concept for Architecture A

1.3 HabEx Baseline Telescope Design

This paper concentrates on the primary mirror for the telescope shown in Figure 3. While the baseline mirror is an open-back Zerodur mirror, other considerations such as mass allocations may require alternative designs. This trade study was conducted to get a better understanding of the driving design parameters for a ULE mirror to meet the HabEx criteria.

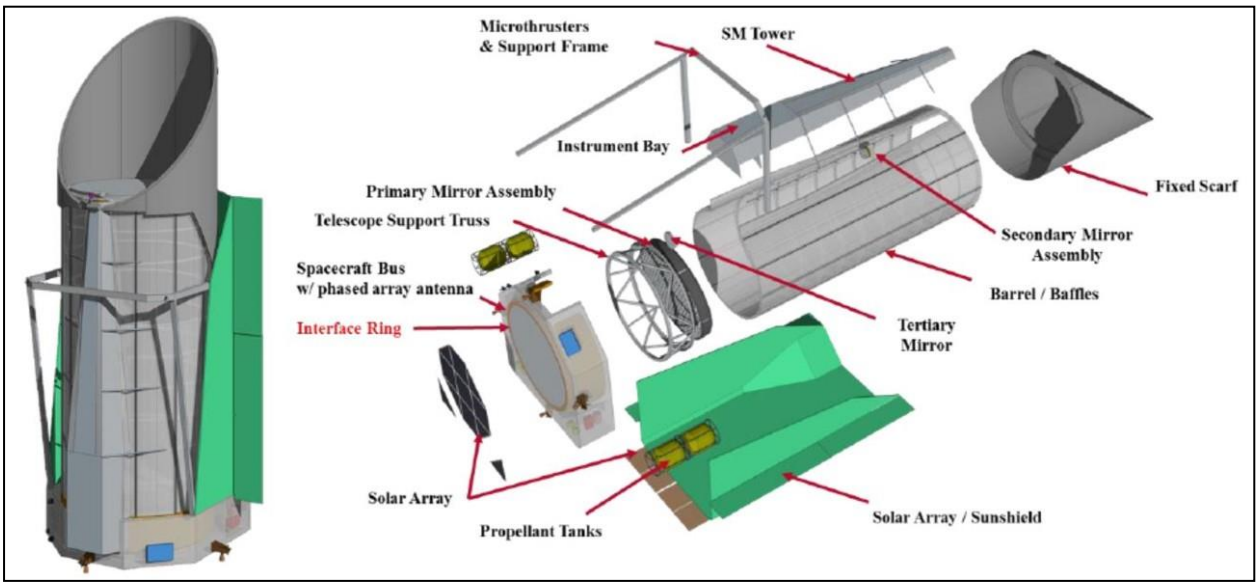

Figure 3: Current Baseline Concept for Telescope portion of satellite

The 4-meter telescope design is off-axis to minimize diffraction, and the station keeping is done using Micro-thrusters, instead of the traditional reaction wheels. The main instrument for planet finding is the advanced coronagraph. Most of the design (mirror performance) requirements are driven by this coronagraph.

1.4 HabEx WFE Stability Specification

The HabEx telescope has a Zernike Polynomial based WFE (wave front error) budget (Figure 4) divided between LOS (line-of-sight) jitter, PM (primary mirror) deformations due to inertial loading, from station keeping, and PM thermal deformations. The LOS jitter is a system level issue (includes secondary mirror and metering structure motions as well a PM motion) and is not addressed in this study. The thermal deformations also depend upon system inputs and are not addressed in this study. The inertial allocation is used to compare trade study results; but remember, the purpose of the study is to understand which parameters influenced WFE, not to find a single point design which meets the specification.

			RSS Allocation	100%	1%	60%	80%	10%
Order				VVC-6 Allowable	LOS	Inertial	Thermal	Reserve
K	N	M	Aberration	[pm rms]	[pm rms]	[pm rms]	[pm rms]	[pm rms]
			TOTAL RMS	416	4	250	333	41
2	1	1	Tilt		0	0	0	0
3	2	0	Power (Defocus)	250	2.5	150	200	24.75
4	2	2	Pri Astigmatism	200	2	120	160	19.8
5	3	1	Pri Coma	175	1.75	105	140	17.325
6	4	0	Pri Spherical	200	2	120	160	19.8
7	3	3	Pri Trefoil	2.6	0.026	1.56	2.08	0.2574
8	4	2	Sec Astigmatism	0.35	0.0035	0.21	0.28	0.03465
9	5	1	Sec Coma	0.35	0.0035	0.21	0.28	0.03465
10	6	0	Sec Spherical	0.35	0.0035	0.21	0.28	0.03465
11	4	4	Pri Tetrafoil	0.35	0.0035	0.21	0.28	0.03465
12	5	3	Sec Trefoil	0.35	0.0035	0.21	0.28	0.03465
13	6	2	Ter Astigmatism	0.1	0.001	0.06	0.08	0.0099
14	7	1	Ter Coma	0.1	0.001	0.06	0.08	0.0099
15	8	0	Ter Spherical	0.1	0.001	0.06	0.08	0.0099
16	5	5	Pri Pentafoil	0.35	0.0035	0.21	0.28	0.03465
17	6	4	Sec Tetrafoil	0.1	0.001	0.06	0.08	0.0099
18	7	3	Ter Trefoil	0.1	0.001	0.06	0.08	0.0099
19	8	2	Qua Astigmatism	0.1	0.001	0.06	0.08	0.0099
20	9	1	Qua Coma	0.1	0.001	0.06	0.08	0.0099
21	10	0	Qua Spherical	0.1	0.001	0.06	0.08	0.0099
22	12	0	Qin Spherical	0.1	0.001	0.06	0.08	0.0099

Figure 4: JPL Initial Tolerance Allocation for Primary Mirror

2. MIRROR TRADE STUDY

The purpose of the trade study was to determine the mirror and suspension system design parameters which influence the mirror's on-orbit performance. The study varied mirror design parameters of core thickness, core cell size, cell wall thickness and facesheet thickness (Figure 5). For most of the study, the reinforcement thicknesses, pad diameter and pad perimeter diameters were held constant. A sub-study compared the influence of no reinforcement (web thickening) and smaller pad size. The sub-study used the same mesh as the reinforced designs. The study also traded support system variations. The hexapod (kinematic) support has three primary variable: number of attachment pads, location of attachment pads and hexapod strut angles relative to the ground plane. This study compared the performance of three attachment pads on mirror with two legs each versus a six pad configuration with one leg on each pad. The pads were attached to the mirror at 100%, 85% and 70% of the mirror's radius (Figure 6). Hexapod stiffness determines the ratio of horizontal modes (X and Y) WFE relative to optical direction (Z) WFE. Two angles are significant in hexapod stiffness. The horizontal angle controls the rotation about Z and together with attachment diameter controls ratio of tilts X and Y to loading in a given direction. As one of the input HabEx design goals is a balanced response in all three directions, the horizontal angle was fixed (maximized the rotation about Z torsional modes) and the hexapod elevation angle (or vertical angle) was varied. The method of varying this parameter in the AMM[4,5] was to increase the hexapod height variable while keeping the upper and lower diameters and plan-view angles the same. (To understand how the modeler works, see the references).

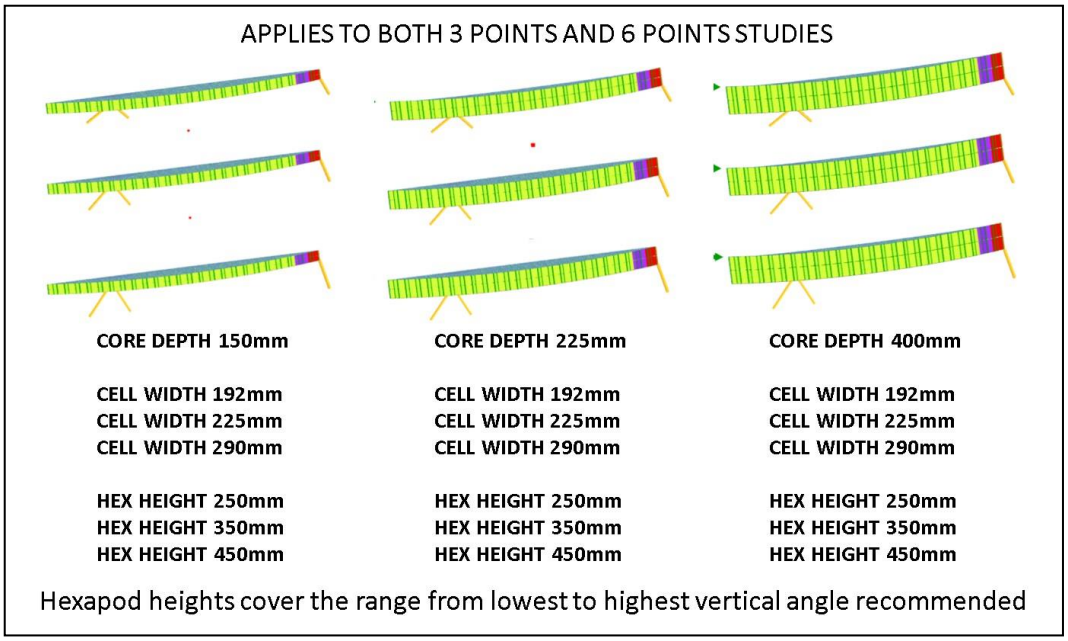

Figure 5: Core Depth and Hexapod Angles

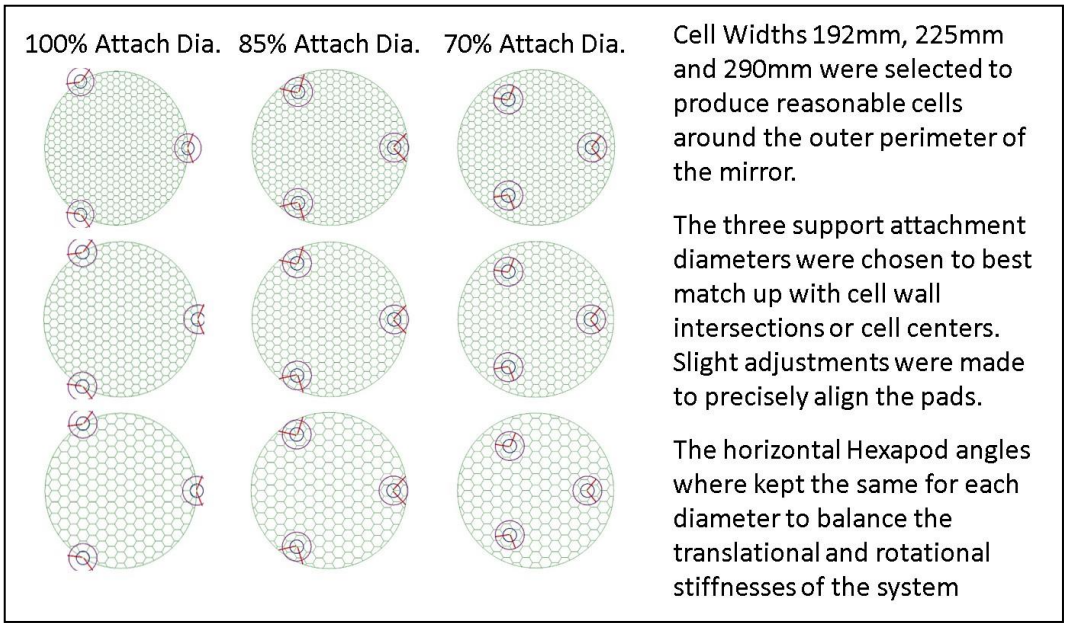

Figure 6: 3 Point Hexapod Geometries

2.1 Scope of Trade Study

The AMM (Arnold Mirror Modeler) software was used to generate separate FEM models of each design point. A separate archive file was generated for each point to permit rerunning or expanding the search about a specific design point. The AMM generates an ANSYS APDL which inputs the model, runs 1g static acceleration loadcases in X,Y and Z directions, post processes these results for mean displacements and RMS surface error for each case, then calculates and plots the first 10 supported modes and the first 10 free-free (mirror only) modes. Each run generates a summary file, and displacement files (of the optical surface nodes only) for input into a Zernike decomposition program. Over 264 cases were created, run and post-processed (in this instance, run thru the Zernike Decomp program) in a two weeks span. The longest time was transferring the results in EXCEL for graphs and tables.

2.2 Three Points Hexapod Results

The results are presented in two formats, graphical (Figure 7) and tabular (Figure 8). The thicker core depths produce higher mounted frequencies but at higher mass. Larger core cells reduce the mass with negligible frequency change. The higher mount diameters increase frequencies. Mount vertical angle has negligible effect on first mode frequencies.

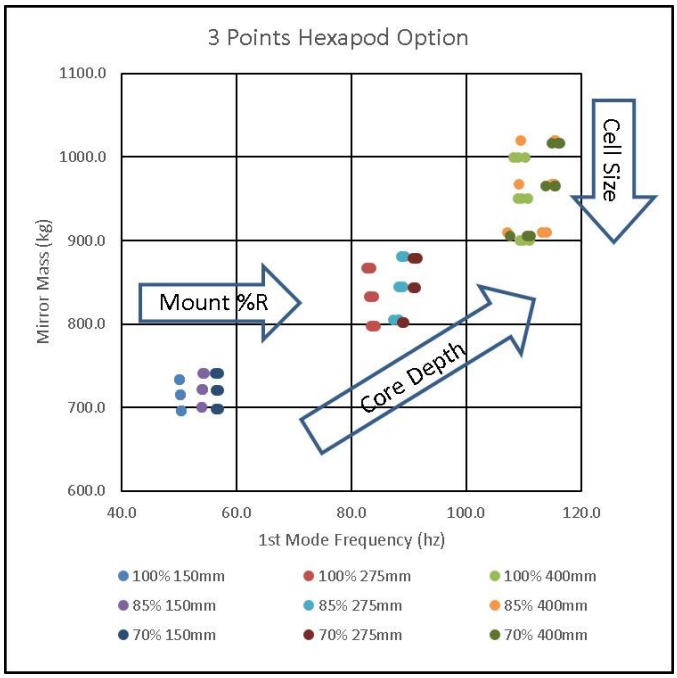

Figure 7: 3 Points Hexapod Mass versus Frequency

100% Diameter

HEX HEIGHT	CORE DEPTH	CELL WIDTH	SUPPORT MASS	SUPPORT 1ST	XYZ RMS
0.250	0.150	0.192	733.7	50.2	3.626E-03
0.350	0.150	0.192	733.7	50.1	3.625E-03
0.450	0.150	0.192	733.7	50.1	3.639E-03
0.250	0.275	0.192	866.6	83.5	1.415E-03
0.350	0.275	0.192	866.6	83.0	1.414E-03
0.450	0.275	0.192	866.6	82.6	1.403E-03
0.250	0.400	0.192	999.5	110.2	8.880E-04
0.350	0.400	0.192	999.5	109.0	9.015E-04
0.450	0.400	0.192	999.5	108.2	9.009E-04
0.250	0.150	0.225	715.2	50.4	3.662E-03
0.350	0.150	0.225	715.2	50.3	3.660E-03
0.450	0.150	0.225	715.2	50.3	3.674E-03
0.250	0.275	0.225	832.9	83.9	1.425E-03
0.350	0.275	0.225	832.9	83.4	1.423E-03
0.450	0.275	0.225	832.9	83.1	1.412E-03
0.250	0.400	0.225	950.5	110.8	8.895E-04
0.350	0.400	0.225	950.5	109.6	9.009E-04
0.450	0.400	0.225	950.5	109.0	8.996E-04
0.250	0.150	0.290	696.0	50.5	3.686E-03
0.350	0.150	0.290	696.0	50.5	3.682E-03
0.450	0.150	0.290	696.0	50.4	3.696E-03
0.250	0.275	0.290	797.8	84.2	1.445E-03
0.350	0.275	0.290	797.8	83.7	1.441E-03
0.450	0.275	0.290	797.8	83.4	1.429E-03
0.250	0.400	0.290	899.6	111.1	9.020E-04
0.350	0.400	0.290	899.6	110.0	9.101E-04
0.450	0.400	0.290	899.6	109.4	9.075E-04

85% Diameter

HEX HEIGHT	CORE DEPTH	CELL WIDTH	SUPPORT MASS	SUPPORT 1ST	XYZ RMS
0.250	0.150	0.192	741.2	54.4	1.895E-03
0.350	0.150	0.192	741.2	54.3	1.900E-03
0.450	0.150	0.192	741.2	54.2	1.903E-03
0.250	0.275	0.192	880.4	88.7	8.171E-04
0.350	0.275	0.192	880.4	89.3	8.178E-04
0.450	0.275	0.192	880.4	88.9	8.175E-04
0.250	0.400	0.192	1019.7	109.5	6.103E-04
0.350	0.400	0.192	1019.7	115.3	5.808E-04
0.450	0.400	0.192	1019.7	115.6	5.746E-04
0.250	0.150	0.225	721.4	54.2	2.022E-03
0.350	0.150	0.225	721.4	54.2	2.027E-03
0.450	0.150	0.225	721.4	54.0	2.032E-03
0.250	0.275	0.225	844.1	88.3	8.675E-04
0.350	0.275	0.225	844.1	89.0	8.619E-04
0.450	0.275	0.225	844.1	88.7	8.542E-04
0.250	0.400	0.225	966.9	109.2	6.285E-04
0.350	0.400	0.225	966.9	114.9	6.006E-04
0.450	0.400	0.225	966.9	115.3	5.940E-04
0.250	0.150	0.290	699.9	54.1	2.030E-03
0.350	0.150	0.290	699.9	54.1	2.028E-03
0.450	0.150	0.290	699.9	54.0	2.027E-03
0.250	0.275	0.290	804.9	87.4	8.874E-04
0.350	0.275	0.290	804.9	88.3	8.764E-04
0.450	0.275	0.290	804.9	88.2	8.665E-04
0.250	0.400	0.290	909.9	107.2	6.326E-04
0.350	0.400	0.290	909.9	113.2	6.108E-04
0.450	0.400	0.290	909.9	113.9	6.032E-04

70% Diameter

HEX HEIGHT	CORE DEPTH	CELL WIDTH	SUPPORT MASS	SUPPORT 1ST	XYZ RMS
0.250	0.150	0.192	740.2	56.9	1.265E-03
0.350	0.150	0.192	740.2	56.6	1.202E-03
0.450	0.150	0.192	740.2	56.4	1.144E-03
0.250	0.275	0.192	878.6	91.5	6.937E-04
0.350	0.275	0.192	878.6	91.2	6.814E-04
0.450	0.275	0.192	878.6	90.8	6.585E-04
0.250	0.400	0.192	1017.1	114.9	5.284E-04
0.350	0.400	0.192	1017.1	116.3	5.287E-04
0.450	0.400	0.192	1017.1	116.0	5.275E-04
0.250	0.150	0.225	720.9	57.0	1.293E-03
0.350	0.150	0.225	720.9	56.7	1.234E-03
0.450	0.150	0.225	720.9	56.5	1.179E-03
0.250	0.275	0.225	843.3	91.2	6.965E-04
0.350	0.275	0.225	843.3	91.0	6.849E-04
0.450	0.275	0.225	843.3	90.7	6.622E-04
0.250	0.400	0.225	965.7	113.8	5.234E-04
0.350	0.400	0.225	965.7	115.5	5.257E-04
0.450	0.400	0.225	965.7	115.4	5.249E-04
0.250	0.150	0.290	698.4	56.9	1.347E-03
0.350	0.150	0.290	698.4	56.7	1.278E-03
0.450	0.150	0.290	698.4	56.6	1.216E-03
0.250	0.275	0.290	802.1	88.8	7.314E-04
0.350	0.275	0.290	802.1	89.2	7.173E-04
0.450	0.275	0.290	802.1	89.0	6.927E-04
0.250	0.400	0.290	905.8	107.6	5.478E-04
0.350	0.400	0.290	905.8	110.6	5.523E-04
0.450	0.400	0.290	905.8	111.2	5.506E-04

Figure 8: Displacement results for 3 Points Hexapods

2.3 Six Points Hexapod Results

The Six Points Hexapods (Figure 9) had similar trends (Figures 10 and 11), core thickness increase mass and stiffness (as measured by first modal frequency) and cell size decreases mass with small stiffness effects. But, the six-point mount results in greater frequency spread with mount geometry changes. Increases in hexapod height (i.e. vertical mount leg angle) decreases first modal frequency.

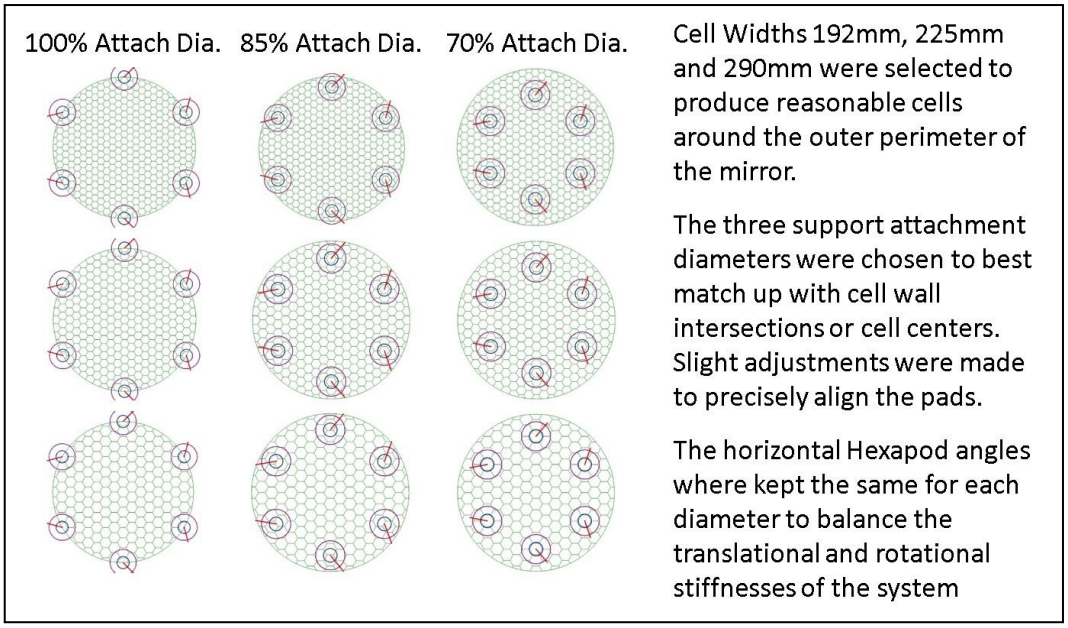

Figure 9: Six Points Hexapod Geometries

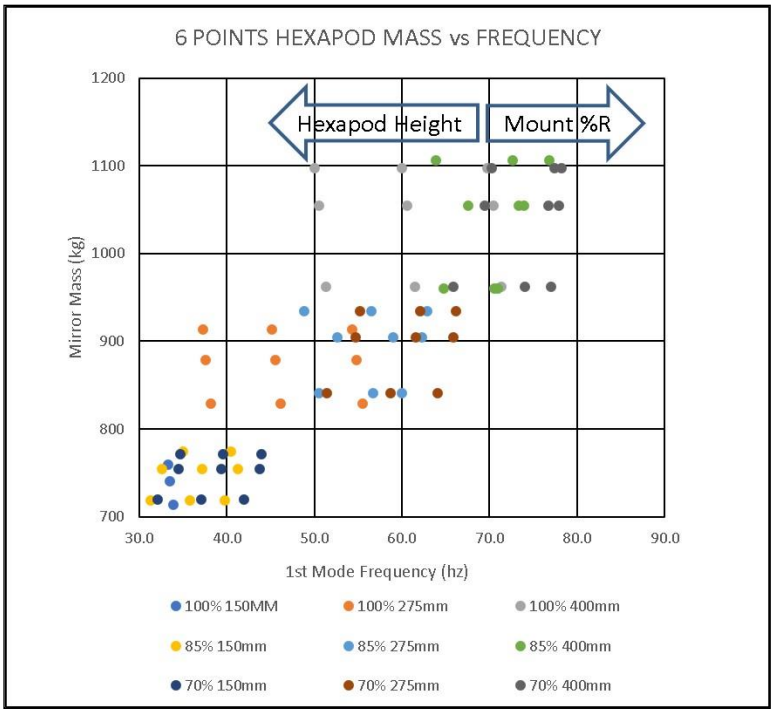

Figure 10: Six Points Hexapod mass versus Frequency

100% Diameter

HEX HEIGHT	CORE DEPTH	CELL WIDTH	SUPPORT MASS	SUPPORT 1ST	XYZ RMS
0.250	0.150	0.192	759.6	33.3	1.754E-02
0.350	0.150	0.192	759.6	27.0	2.509E-02
0.450	0.150	0.192	759.6	22.2	3.276E-02
0.250	0.275	0.192	913.6	54.3	6.193E-03
0.350	0.275	0.192	913.6	45.2	8.841E-03
0.450	0.275	0.192	913.6	37.3	1.160E-02
0.250	0.400	0.192	1067.6	69.8	3.474E-03
0.350	0.400	0.192	1067.6	60.0	4.895E-03
0.450	0.400	0.192	1067.6	50.1	6.411E-03
0.250	0.150	0.225	740.2	33.5	1.749E-02
0.350	0.150	0.225	740.2	27.2	2.501E-02
0.450	0.150	0.225	740.2	22.3	3.265E-02
0.250	0.275	0.225	878.1	54.8	6.150E-03
0.350	0.275	0.225	878.1	45.6	8.767E-03
0.450	0.275	0.225	878.1	37.6	1.149E-02
0.250	0.400	0.225	1016.0	70.4	3.447E-03
0.350	0.400	0.225	1016.0	60.6	4.847E-03
0.450	0.400	0.225	1016.0	50.5	6.341E-03
0.250	0.150	0.290	713.4	33.9	1.756E-02
0.350	0.150	0.290	713.4	27.5	2.507E-02
0.450	0.150	0.290	713.4	22.5	3.272E-02
0.250	0.275	0.290	829.2	55.5	6.129E-03
0.350	0.275	0.290	829.2	46.2	8.723E-03
0.450	0.275	0.290	829.2	38.2	1.142E-02
0.250	0.400	0.290	945.0	71.4	3.423E-03
0.350	0.400	0.290	945.0	61.5	4.802E-03
0.450	0.400	0.290	945.0	51.3	6.272E-03

85% Diameter

HEX HEIGHT	CORE DEPTH	CELL WIDTH	SUPPORT MASS	SUPPORT 1ST	XYZ RMS
0.250	0.150	0.192	773.9	40.4	1.094E-02
0.350	0.150	0.192	773.9	35.0	1.584E-02
0.450	0.150	0.192	773.9	29.8	2.083E-02
0.250	0.275	0.192	939.9	62.8	3.981E-03
0.350	0.275	0.192	939.9	56.5	5.755E-03
0.450	0.275	0.192	939.9	48.9	7.598E-03
0.250	0.400	0.192	1105.9	76.8	2.275E-03
0.350	0.400	0.192	1105.9	72.6	3.271E-03
0.450	0.400	0.192	1105.9	63.9	4.315E-03
0.250	0.150	0.225	754.7	41.3	9.516E-03
0.350	0.150	0.225	754.7	37.2	1.390E-02
0.450	0.150	0.225	754.7	32.6	1.837E-02
0.250	0.275	0.225	904.7	62.3	3.536E-03
0.350	0.275	0.225	904.7	59.0	5.127E-03
0.450	0.275	0.225	904.7	52.6	6.795E-03
0.250	0.400	0.225	1054.8	73.3	2.044E-03
0.350	0.400	0.225	1054.8	73.9	2.980E-03
0.450	0.400	0.225	1054.8	67.6	3.936E-03
0.250	0.150	0.290	718.9	39.8	1.054E-02
0.350	0.150	0.290	718.9	35.8	1.536E-02
0.450	0.150	0.290	718.9	31.3	2.028E-02
0.250	0.275	0.290	839.3	60.0	3.921E-03
0.350	0.275	0.290	839.3	56.7	5.651E-03
0.450	0.275	0.290	839.3	50.5	7.466E-03
0.250	0.400	0.290	959.6	70.6	2.278E-03
0.350	0.400	0.290	959.6	71.0	3.296E-03
0.450	0.400	0.290	959.6	64.8	4.334E-03

70% Diameter

HEX HEIGHT	CORE DEPTH	CELL WIDTH	SUPPORT MASS	SUPPORT 1ST	XYZ RMS
0.250	0.150	0.192	770.8	44.0	8.112E-03
0.350	0.150	0.192	770.8	39.6	1.188E-02
0.450	0.150	0.192	770.8	34.7	1.572E-02
0.250	0.275	0.192	934.2	66.2	3.066E-03
0.350	0.275	0.192	934.2	62.1	4.503E-03
0.450	0.275	0.192	934.2	55.2	5.995E-03
0.250	0.400	0.192	1097.6	78.2	1.778E-03
0.350	0.400	0.192	1097.6	77.5	2.652E-03
0.450	0.400	0.192	1097.6	70.3	3.542E-03
0.250	0.150	0.225	754.7	43.8	8.231E-03
0.350	0.150	0.225	754.7	39.4	1.205E-02
0.450	0.150	0.225	754.7	34.5	1.593E-02
0.250	0.275	0.225	904.7	65.9	3.129E-03
0.350	0.275	0.225	904.7	61.6	4.592E-03
0.450	0.275	0.225	904.7	54.7	6.107E-03
0.250	0.400	0.225	1054.8	77.9	1.821E-03
0.350	0.400	0.225	1054.8	76.8	2.716E-03
0.450	0.400	0.225	1054.8	69.5	3.626E-03
0.250	0.150	0.290	719.8	42.0	9.615E-03
0.350	0.150	0.290	719.8	37.1	1.403E-02
0.450	0.150	0.290	719.8	32.1	1.851E-02
0.250	0.275	0.290	840.8	64.1	3.616E-03
0.350	0.275	0.290	840.8	58.7	5.280E-03
0.450	0.275	0.290	840.8	51.4	6.998E-03
0.250	0.400	0.290	961.9	77.1	2.108E-03
0.350	0.400	0.290	961.9	74.0	3.100E-03
0.450	0.400	0.290	961.9	65.9	4.115E-03

Figure 11: Displacement results for Six Points Hexapods

3. INERTIAL DEFORMATION

To our knowledge, inertial deformation may be a new performance metric and is defined as the mirror deformation produced by an acceleration. For example, gravity sag is the deformation produced when the mirror (on its mount) is exposed to a 1-G acceleration. On-orbit, inertial deformation is the response of the mirror (reacting against its mount) when it is exposed to accelerations from sources such slews, solar wind, reaction wheel noise, etc. And, can be modeled simply as gravity sag deformation scaled by the ratio of accelerations. In the case of HabEx, point stability will be maintained via micro-thrusters with a specified noise of 0.1 micro-Newton (~0.01 micro-G). This error is then decomposed into Zernike polynomials and compared to the specified error budget.

3.1 Analysis Process

Due to numerical accuracy inherent in finite element modeling and types of models and elements used, all analyses were performed in meters at one gravity (9.802 m/s^2), the displacements were then scaled to the appropriate levels. The load-cases were unit 1 g accelerations in the three axes (X, Y and Z) (Figure 12). These displacements were output into individual files and then input into a purpose-built Zernike Decomposition program which processed each load-case. Zernikes were scaled to the appropriate units then RSSed (square root of the sum of squares) together (Figure 13) to be compared to the tolerance table. The dedicated program created a results file for insertion into EXCEL tables reported in Figures 14, 15 and 21.

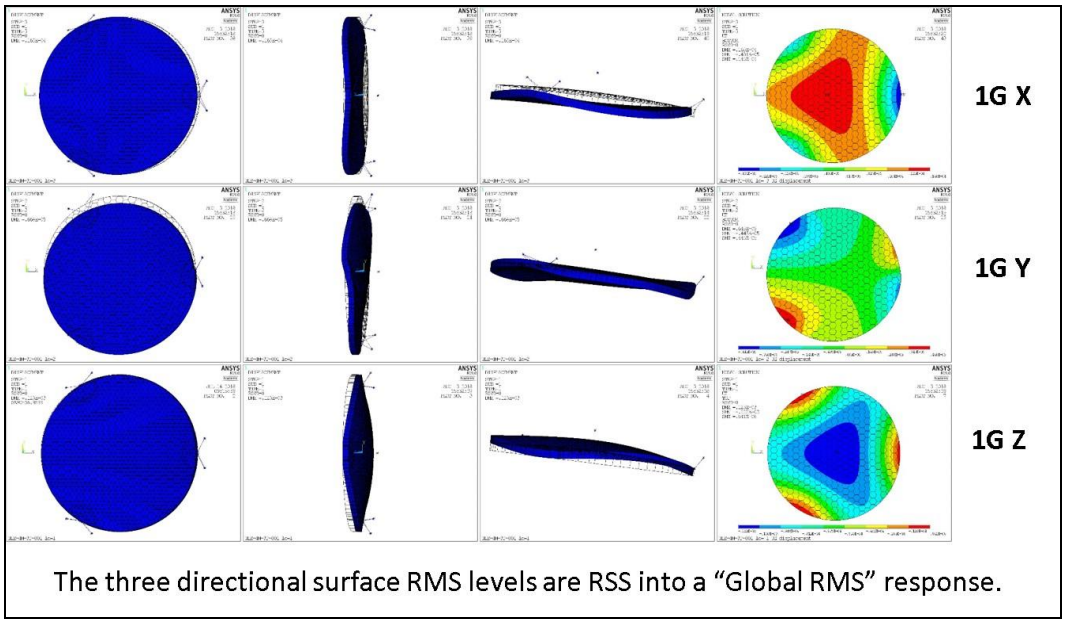

Figure 12: Typical Static Load-Case Results

Sigfit RSS Comparison Title: FST-007-11-10

Order			Aberration	(PICO-METER/MICRO-G)				
K	N	M		X	Y	Z	RSS	Tolerance
1	0	0	Bias	0.290	0.000	4.619	4.628	0.00
2	1	1	Tilt	0.562	0.491	0.164	0.764	0.00
3	2	0	Power (Defocus)	0.271	0.000	2.319	2.335	150.00
4	2	2	Pri Astigmatism	2.235	2.174	0.348	3.137	120.00
5	3	1	Pri Coma	0.015	0.018	0.040	0.047	105.00
6	4	0	Pri Spherical	0.023	0.000	0.166	0.168	120.00
7	3	3	Pri Trefoil	0.366	0.023	3.072	3.094	1.56
8	4	2	Sec Astigmatism	0.104	0.103	0.030	0.149	0.21
9	5	1	Sec Coma	0.007	0.005	0.004	0.009	0.21
10	6	0	Sec Spherical	0.010	0.000	0.099	0.099	0.21
11	4	4	Pri Tetrafoil	0.222	0.211	0.024	0.307	0.21
12	5	3	Sec Trefoil	0.045	0.005	0.357	0.360	0.21
13	6	2	Ter Astigmatism	0.010	0.010	0.003	0.015	0.06
14	7	1	Ter Coma	0.007	0.007	0.006	0.011	0.06
15	8	0	Ter Spherical	0.018	0.076	0.255	0.266	0.21
16	5	5	Pri Pentafoil	0.250	0.244	0.054	0.354	0.06
17	6	4	Sec Tetrafoil	0.027	0.022	0.001	0.035	0.06
18	7	3	Ter Trefoil	0.009	0.001	0.066	0.067	0.06
19	8	2	Qua Astigmatism	0.004	0.004	0.004	0.007	0.06
20	9	1	Qua Coma	0.005	0.080	0.006	0.080	0.06
21	10	0	Qua Spherical	0.000	0.005	0.001	0.005	0.06
22	12	0	Qui Spherical	0.036	0.000	0.533	0.534	0.06

Figure 13: RSS of X,Y,Z Zernike Polynomials

3.2 Core Depth Trade Study

This portion of the study looked at one cell size and the 100% mount diameter. The main result was that none of the variations met the WFE error budget specification in all terms. But, the thicker and stiffer the mirror, the better.

ZERNIKES	WFE Tol	3 Point Mount Error [pm rms]			6 Point Mount Error [pm rms]		
K N M	[pm rms]	150 mm	275 mm	400 mm	150 mm	275 mm	400 mm
3 2 0 Power (Defocus)	150.00	11.376	4.238	2.335	11.067	3.822	1.939
4 2 2 Pri Astigmatism	120.00	1.128	3.037	3.033	60.995	19.948	9.967
5 3 1 Pri Coma	105.00	0.252	0.083	0.047	0.253	0.104	0.071
6 4 0 Pri Spherical	120.00	0.520	0.258	0.166	0.797	0.373	0.233
7 3 3 Pri Trefoil	1.56	14.761	5.431	3.094	1.597	1.225	1.025
8 4 2 Sec Astigmatism	0.21	0.051	0.120	0.144	2.718	1.094	0.669
9 5 1 Sec Coma	0.21	0.022	0.004	0.009	0.017	0.007	0.016
10 6 0 Sec Spherical	0.21	0.334	0.146	0.097	0.252	0.132	0.102
11 4 4 Pri Tetrafoil	0.21	0.491	0.384	0.302	5.996	2.336	1.404
12 5 3 Sec Trefoil	0.21	1.171	0.527	0.352	0.120	0.108	0.100
13 6 2 Ter Astigmatism	0.06	0.029	0.016	0.014	0.224	0.151	0.124
14 7 1 Ter Coma	0.06	0.026	0.011	0.011	0.019	0.010	0.012
15 8 0 Ter Spherical	0.06	1.213	0.454	0.266	0.671	0.295	0.208
16 5 5 Pri Pentafoil	0.21	0.365	0.377	0.342	0.693	0.528	0.443
17 6 4 Sec Tetrafoil	0.06	0.055	0.047	0.035	0.749	0.418	0.318
18 7 3 Ter Trefoil	0.06	0.044	0.065	0.064	0.016	0.008	0.003
19 8 2 Qua Astigmatism	0.06	0.012	0.005	0.007	0.033	0.022	0.017
20 9 1 Qua Coma	0.06	0.097	0.088	0.078	0.182	0.084	0.053
21 10 2 Qua Astigmatism	0.06	0.003	0.003	0.005	0.003	0.002	0.003
22 12 0 Qin Spherical	0.06	2.613	0.943	0.536	1.350	0.540	0.373

Figure 14: Processed results of Core Depth Study

3.3 Mount Diameter Trade Study

This portion looked at the 400mm Core Depth and 290mm Cell Size and varied the mount diameters for 3 and 6 point cases. Different mount pad and radial distance locations result is different Zernike polynomial WFE distributions.

ZERNIKES	WFE Tol	3 Point Mount Error [pm rms]			6 Point Mount Error [pm rms]		
K N M	[pm rms]	100%	85%	70%	100%	85%	70%
3 2 0 Power (Defocus)	150.00	2.599	0.632	0.834	2.226	0.083	0.633
4 2 2 Pri Astigmatism	120.00	2.876	2.813	2.633	9.527	4.727	5.050
5 3 1 Pri Coma	105.00	0.050	0.231	0.491	0.069	0.357	0.478
6 4 0 Pri Spherical	120.00	0.031	0.365	0.244	0.136	0.451	0.325
7 3 3 Pri Trefoil	1.56	3.129	2.397	1.608	0.969	0.788	0.589
8 4 2 Sec Astigmatism	0.21	0.135	0.361	0.639	0.684	1.371	1.807
9 5 1 Sec Coma	0.21	0.013	0.048	0.047	0.021	0.039	0.023
10 6 0 Sec Spherical	0.21	0.060	0.006	0.258	0.067	0.023	0.222
11 4 4 Pri Tetrafoil	0.21	0.289	0.085	0.022	1.457	0.953	0.895
12 5 3 Sec Trefoil	0.21	0.397	1.169	1.243	0.093	0.182	0.188
13 6 2 Ter Astigmatism	0.06	0.019	0.012	0.166	0.150	0.064	0.361
14 7 1 Ter Coma	0.06	0.013	0.023	0.064	0.017	0.041	0.066
15 8 0 Ter Spherical	0.06	0.382	0.208	0.174	0.278	0.160	0.083
16 5 5 Pri Pentafoil	0.21	0.345	0.247	0.151	0.437	0.319	0.284
17 6 4 Sec Tetrafoil	0.06	0.029	0.050	0.046	0.354	0.810	0.971
18 7 3 Ter Trefoil	0.06	0.083	0.122	0.509	0.002	0.030	0.051
19 8 2 Qua Astigmatism	0.06	0.009	0.038	0.020	0.015	0.169	0.127
20 9 1 Qua Coma	0.06	0.077	0.039	0.027	0.068	0.013	0.018
21 10 2 Qua Astigmatism	0.06	0.009	0.005	0.022	0.005	0.002	0.014
22 12 0 Qin Spherical	0.06	0.857	0.629	0.491	0.639	0.484	0.414

Figure15: Mount Diameter Trade Study

3.4 Trade Study on Back Profiles

This study investigated the influence of the back profile. Based upon earlier open-backed results we were expecting an effect. But, for the closed back design, the back-sheet seems to have negated the benefit of a deeper outer zone.

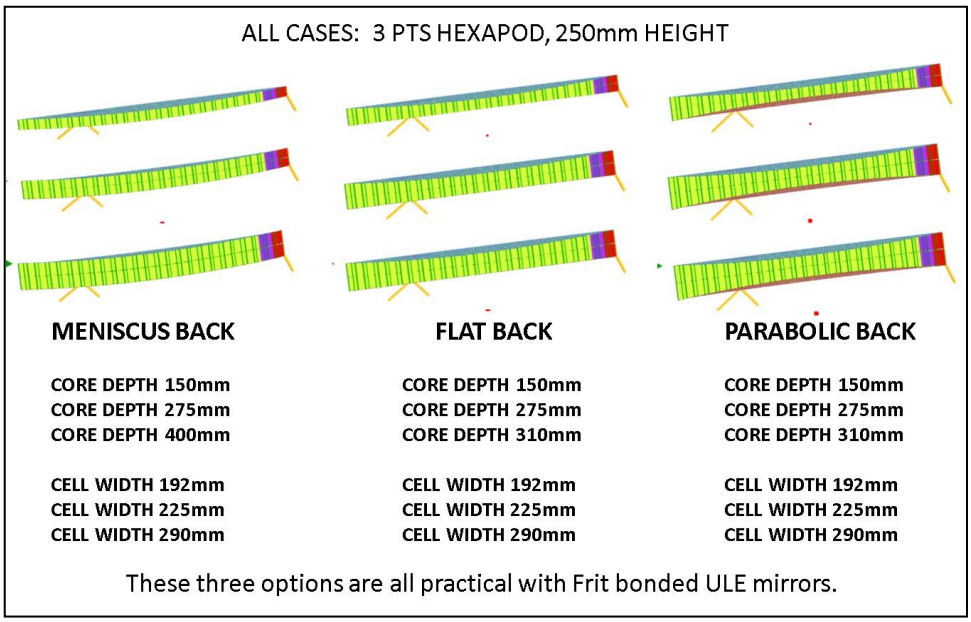

Figure 16: Basic Parameters looked at in Back Profile Study.

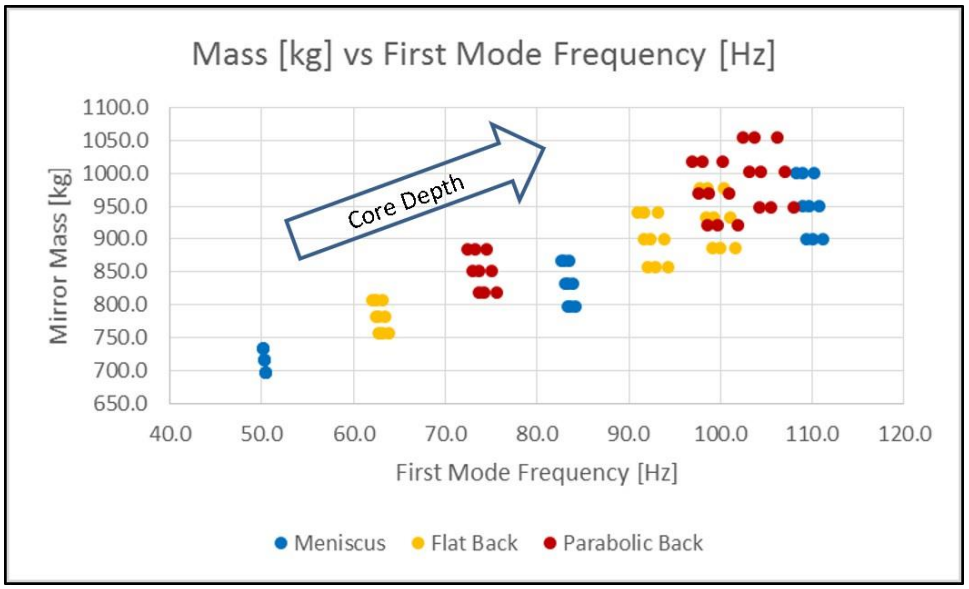

Figure 17: Mass versus Frequency for Back Profiles.

MENISCUS

HEX HEIGHT	CORE DEPTH	CELL WIDTH	SUPPORT MASS	SUPPORT 1ST	XYZ RMS
0.250	0.150	0.192	733.7	50.2	3.626E-03
0.350	0.150	0.192	733.7	50.1	3.625E-03
0.450	0.150	0.192	733.7	50.1	3.639E-03
0.250	0.275	0.192	866.6	83.5	1.415E-03
0.350	0.275	0.192	866.6	83.0	1.414E-03
0.450	0.275	0.192	866.6	82.6	1.403E-03
0.250	0.400	0.192	999.5	110.2	8.880E-04
0.350	0.400	0.192	999.5	109.0	9.015E-04
0.450	0.400	0.192	999.5	108.2	9.009E-04
0.250	0.150	0.225	715.2	50.4	3.662E-03
0.350	0.150	0.225	715.2	50.3	3.660E-03
0.450	0.150	0.225	715.2	50.3	3.674E-03
0.250	0.275	0.225	832.9	83.9	1.425E-03
0.350	0.275	0.225	832.9	83.4	1.423E-03
0.450	0.275	0.225	832.9	83.1	1.412E-03
0.250	0.400	0.225	950.5	110.8	8.895E-04
0.350	0.400	0.225	950.5	109.6	9.009E-04
0.450	0.400	0.225	950.5	109.0	8.996E-04
0.250	0.150	0.290	696.0	50.5	3.686E-03
0.350	0.150	0.290	696.0	50.5	3.682E-03
0.450	0.150	0.290	696.0	50.4	3.696E-03
0.250	0.275	0.290	797.8	84.2	1.445E-03
0.350	0.275	0.290	797.8	83.7	1.441E-03
0.450	0.275	0.290	797.8	83.4	1.429E-03
0.250	0.400	0.290	899.6	111.1	9.020E-04
0.350	0.400	0.290	899.6	110.0	9.101E-04
0.450	0.400	0.290	899.6	109.4	9.075E-04

FLAT BACK

HEX HEIGHT	CORE DEPTH	CELL WIDTH	SUPPORT MASS	SUPPORT 1ST	XYZ RMS
0.250	0.150	0.192	807.8	63.2	4.168E-03
0.350	0.150	0.192	807.8	62.5	4.300E-03
0.450	0.150	0.192	807.8	62.1	4.382E-03
0.250	0.275	0.192	940.7	93.2	1.911E-03
0.350	0.275	0.192	940.7	91.7	1.978E-03
0.450	0.275	0.192	940.7	90.9	2.026E-03
0.250	0.310	0.192	977.9	100.4	1.647E-03
0.350	0.310	0.192	977.9	98.6	1.703E-03
0.450	0.310	0.192	977.9	97.7	1.745E-03
0.250	0.150	0.225	782.0	63.5	4.103E-03
0.350	0.150	0.225	782.0	62.8	4.228E-03
0.450	0.150	0.225	782.0	62.5	4.306E-03
0.250	0.275	0.225	899.7	93.9	1.884E-03
0.350	0.275	0.225	899.7	92.3	1.946E-03
0.450	0.275	0.225	899.7	91.6	1.991E-03
0.250	0.310	0.225	932.6	101.1	1.625E-03
0.350	0.310	0.225	932.6	99.3	1.676E-03
0.450	0.310	0.225	932.6	98.5	1.714E-03
0.250	0.150	0.290	756.3	63.8	3.937E-03
0.350	0.150	0.290	756.3	63.1	4.052E-03
0.450	0.150	0.290	756.3	62.8	4.125E-03
0.250	0.275	0.290	858.1	94.3	1.818E-03
0.350	0.275	0.290	858.1	92.9	1.872E-03
0.450	0.275	0.290	858.1	92.1	1.912E-03
0.250	0.310	0.290	886.6	101.6	1.569E-03
0.350	0.310	0.290	886.6	99.9	1.613E-03
0.450	0.310	0.290	886.6	99.1	1.647E-03

PARABOLIC BACK

HEX HEIGHT	CORE DEPTH	CELL WIDTH	SUPPORT MASS	SUPPORT 1ST	XYZ RMS
0.250	0.150	0.192	883.9	74.5	2.647E-03
0.350	0.150	0.192	883.9	73.2	2.805E-03
0.450	0.150	0.192	883.9	72.5	2.906E-03
0.250	0.275	0.192	1016.9	100.3	1.438E-03
0.350	0.275	0.192	1016.9	98.0	1.520E-03
0.450	0.275	0.192	1016.9	96.9	1.578E-03
0.250	0.310	0.192	1054.1	106.2	1.278E-03
0.350	0.310	0.192	1054.1	103.7	1.346E-03
0.450	0.310	0.192	1054.1	102.4	1.397E-03
0.250	0.150	0.225	850.8	75.0	2.611E-03
0.350	0.150	0.225	850.8	73.7	2.761E-03
0.450	0.150	0.225	850.8	73.0	2.858E-03
0.250	0.275	0.225	968.5	101.0	1.423E-03
0.350	0.275	0.225	968.5	98.7	1.498E-03
0.450	0.275	0.225	968.5	97.6	1.552E-03
0.250	0.310	0.225	1001.4	107.0	1.265E-03
0.350	0.310	0.225	1001.4	104.4	1.327E-03
0.450	0.310	0.225	1001.4	103.2	1.374E-03
0.250	0.150	0.290	818.6	75.7	2.502E-03
0.350	0.150	0.290	818.6	74.3	2.645E-03
0.450	0.150	0.290	818.6	73.7	2.738E-03
0.250	0.275	0.290	920.3	101.9	1.368E-03
0.350	0.275	0.290	920.3	99.7	1.439E-03
0.450	0.275	0.290	920.3	98.6	1.490E-03
0.250	0.310	0.290	948.8	108.0	1.217E-03
0.350	0.310	0.290	948.8	105.5	1.275E-03
0.450	0.310	0.290	948.8	104.3	1.319E-03

Figure 18: Results of Back Surface Profile Study

3.5 Local Reinforcement Study

Local reinforcement usually refers to localized increases in core web thicknesses. With ULE mirrors in particular, waterjet cutting of the core makes this relatively easy to do. The front and back sheets are usually uniform thickness. There is a mass penalty for this feature, but launch loads and local stresses under pads become a serious issue as the mirrors become lighter and thinner sections. Most of the cases used a fixed reinforcement thickness pattern and pad and perimeter diameters. To see if there was any significant benefit to this local reinforcement, a series of runs were made using the same mesh as reinforced, but keeping all core webs uniform (minimal) thickness (Figure 19). While the previous open back design study indicated that local reinforcement provided a significant benefit, the closed back design does not indicate the same advantage - back plate seems to have eliminated much of the need for local reinforcement.

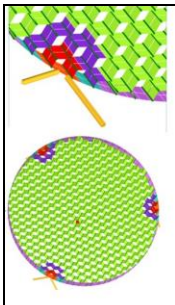

RUN ID	UPPER DIA	HEX HEIGHT	CORE DEPTH	CELL WIDTH	PAD DIA	PERIM DIA	SUPPORT MASS	SUPPORT 1ST	XYZ RMS
ULE-4M-3P-019	4.040	0.250	0.150	0.290	0.350	0.750	696.0	50.5	3.686E-03
ULE-4M-3P-019N	4.040	0.250	0.150	0.290	0.350	0.750	677.0	49.7	3.826E-03
ULE-4M-3P-019SP	4.040	0.250	0.150	0.290	0.175	0.350	677.0	48.5	4.092E-03
ULE-4M-3P-046	3.430	0.250	0.150	0.290	0.350	0.750	699.9	54.1	2.030E-03
ULE-4M-3P-046N	3.430	0.250	0.150	0.290	0.350	0.750	677.0	52.5	2.172E-03
ULE-4M-3P-046SP	3.430	0.250	0.150	0.290	0.175	0.350	677.0	50.2	2.411E-03
ULE-4M-3P-073	2.820	0.250	0.150	0.290	0.350	0.750	698.4	56.9	1.347E-03
ULE-4M-3P-073N	2.820	0.250	0.150	0.290	0.350	0.750	677.0	54.7	1.350E-03
ULE-4M-3P-073SP	2.820	0.250	0.150	0.290	0.175	0.350	677.0	51.4	1.506E-03

The run id with no letter is the reinforced core case.
The run id with letter N is the same mesh, but no additional web thickness.
The run id with the letters SP has smaller pad diameters and no additional web thickness.

Figure 19: Local Reinforcement Study

3.6 Hexapod Leg Stiffness Study

All the previous runs used a common strut stiffness value. In order to see if that value was influencing the results, a short parametric study was done using just one geometry case from each mount diameter and 3 and 6 point configurations. The strut stiffness was reduced by two orders of magnitude for each step. The result (Figure 20) showed that once a certain threshold was reached, the actual leg stiffness did not influence the results.

	UPPER	HEX	LEG	CORE	CELL	SUPPORT	SUPPORT	XYZ
RUN ID	DIA	HEIGHT	STIFF	DEPTH	WIDTH	MASS	1ST	RMS
ULE-4M-3P-001	4.040	0.250	8.E+11	0.150	0.192	733.7	50.2	3.626E-03
ULE-4M-3P-001A	4.040	0.250	8.E+09	0.150	0.192	733.7	50.1	3.628E-03
ULE-4M-3P-001B	4.040	0.250	8.E+07	0.150	0.192	733.7	41.69	4.469E-03
ULE-4M-3P-028	3.430	0.250	8.E+11	0.150	0.192	741.2	54.4	1.895E-03
ULE-4M-3P-028A	3.430	0.250	8.E+09	0.150	0.192	741.2	54.2	1.906E-03
ULE-4M-3P-028B	3.430	0.250	8.E+07	0.150	0.192	741.2	35.1	8.828E-03
ULE-4M-3P-055	2.820	0.250	8.E+11	0.150	0.192	740.2	56.9	1.265E-03
ULE-4M-3P-055A	2.820	0.250	8.E+09	0.150	0.192	740.2	56.7	1.256E-03
ULE-4M-3P-055B	2.820	0.250	8.E+07	0.150	0.192	740.2	39.4	6.701E-03
ULE-4M-6P-001	4.040	0.250	8.E+11	0.150	0.192	759.6	33.3	1.754E-02
ULE-4M-6P-001A	4.040	0.250	8.E+09	0.150	0.192	759.6	33.2	1.762E-02
ULE-4M-6P-001B	4.040	0.250	8.E+07	0.150	0.192	759.6	26.8	2.563E-02
ULE-4M-6P-028	3.430	0.250	8.E+11	0.150	0.192	773.9	40.4	1.094E-02
ULE-4M-6P-028A	3.430	0.250	8.E+09	0.150	0.192	773.9	40.3	1.103E-02
ULE-4M-6P-028B	3.430	0.250	8.E+07	0.150	0.192	773.9	28.2	2.047E-02
ULE-4M-6P-055	2.820	0.250	8.E+11	0.150	0.192	770.8	44.0	8.112E-03
ULE-4M-6P-055A	2.820	0.250	8.E+09	0.150	0.192	770.8	43.7	8.234E-03
ULE-4M-6P-055B	2.820	0.250	8.E+07	0.150	0.192	770.8	25.8	2.052E-02

Figure 20: Hexapod Leg Stiffness Results

3.7 Facesheet Thickness Study

Finally, a study of the effect of the facesheet on the mid-frequency Zernikes was done. In the second row of Figure 21, the first number is the thickness of the front-sheet and the second number is the thickness of the back-sheet. Ignoring quilting, no significant improvement is provided by increases up to 13mm for either the front only or both plates.

ZERNIKES	WFE Tol	400 Core 190 Cell 100% Attach Error [pm rms]						
K N M	[pm rms]	10 10	11 10	12 10	13 10	11 11	12 12	13 13
3 2 0 Power (Defocus)	150.00	2.335	2.335	2.341	2.354	2.354	2.379	2.407
4 2 2 Pri Astigmatism	120.00	3.033	3.137	3.241	3.345	2.949	2.880	2.822
5 3 1 Pri Coma	105.00	0.047	0.047	0.046	0.046	0.047	0.047	0.048
6 4 0 Pri Spherical	120.00	0.166	0.168	0.170	0.172	0.168	0.169	0.171
7 3 3 Pri Trefoil	1.56	3.094	3.094	3.102	3.116	3.115	3.142	3.175
8 4 2 Sec Astigmatism	0.21	0.144	0.149	0.154	0.159	0.141	0.138	0.135
9 5 1 Sec Coma	0.21	0.009	0.009	0.010	0.011	0.009	0.010	0.010
10 6 0 Sec Spherical	0.21	0.097	0.099	0.101	0.103	0.101	0.105	0.109
11 4 4 Pri Tetrafoil	0.21	0.302	0.307	0.312	0.318	0.291	0.282	0.273
12 5 3 Sec Trefoil	0.21	0.352	0.360	0.368	0.376	0.361	0.371	0.382
13 6 2 Ter Astigmatism	0.06	0.014	0.015	0.015	0.016	0.015	0.016	0.016
14 7 1 Ter Coma	0.06	0.011	0.011	0.012	0.012	0.011	0.012	0.012
15 8 0 Ter Spherical	0.06	0.266	0.266	0.267	0.269	0.269	0.272	0.276
16 5 5 Pri Pentafoil	0.21	0.342	0.354	0.365	0.376	0.342	0.342	0.342
17 6 4 Sec Tetrafoil	0.06	0.035	0.035	0.035	0.035	0.034	0.032	0.031
18 7 3 Ter Trefoil	0.06	0.064	0.067	0.070	0.072	0.069	0.074	0.079
19 8 2 Qua Astigmatism	0.06	0.007	0.007	0.007	0.007	0.007	0.006	0.006
20 9 1 Qua Coma	0.06	0.078	0.080	0.083	0.085	0.079	0.080	0.081
21 10 2 Qua Astigmatism	0.06	0.005	0.005	0.005	0.005	0.005	0.005	0.005
22 12 0 Qin Spherical	0.06	0.536	0.534	0.534	0.535	0.541	0.547	0.554

Figure 21: Facesheet Thickness Study Results

4. CONCLUSIONS

The Habitable Exoplanet Observatory (HabEx) mission requires a telescope whose optical wavefront has ultra-stable mid-spatial frequency error to enable coronagraphy of exo-Earth class planets. While mass and stiffness are still important design parameters, for coronagraphy, the more important metric is inertial WFE, i.e. the response of the mirror to on-orbit acceleration noise. While an open-back Zerodur mirror is the current baseline, this paper summarizes a series of trade studies for a potential alternative closed-back ULE design. The study looked at over 264 design variations using the Arnold Mirror Modeler and ANSYS© to investigate the influence of various design elements. As expected, the stiffer the mirror, the better its total rms inertial deformation. But, the distribution of that deformation (i.e. its decomposition into Zernike polynomials) varies with mount configuration (3 vs 6 pads, radial pad location, and strut angle). While previous studies indicated that back shape and local reinforcement were beneficial for open-back mirrors, their benefit was smaller for the closed-back mirrors in this trade study. One conclusion is that the back-sheet eliminates the need for local reinforcement and edge support.

REFERENCES

[1] Stahl, H. Phillip, "Overview and performance predictions of the baseline 4-meter telescope concept design for habitable-zone exoplanet Observatory",

[2] Arnold, W.R., and Stahl, H. Phillip, "Structural design of a 4-meter off-axis space telescope for the Habitable-zone Exoplanet Direct Imaging Mission", SPIE 10398-7 (2017).

[3] Arnold, W.R., "AMTD design process," NASA/ SPIE Mirror Technology Days, Albuquerque, NM (2014).

[4] Arnold, W.R., Etal, "Next Generation lightweight mirror modeling software", SPIE Opto-mechanical Engineering 2013, San Diego, CA SPIE 8836-15 (2013).

[5] Arnold, W.R., Etal, "Integration of mirror design with suspension system using NASA's new mirror modeling software", SPIE Opto-mechanical Engineering 2013, San Diego, CA SPIE 8836-17 (2013).

[6] Arnold, W.R., Etal, "Next Generation lightweight mirror modeling software", NASA Mirror Tech Days, Redondo Beach, CA (2013).